

DEVELOPMENT OF A NONLINEAR MULTI-INPUT/MULTI-OUTPUT MODEL FOR THE VINCENT THOMAS BRIDGE UNDER EARTHQUAKE EXCITATIONS

Andrew W SMYTH¹, Sami F MASRI², Ahmed M ABDEL-GHAFFAR³ And Robert N NIGBOR⁴

SUMMARY

The system identification and damage detection of long-span structures has been an area of considerable interest due to the critical role such structures often play in civil infrastructure systems. Because of their inherent length, such structures must be viewed as having multiple inputs at the base during strong-ground motions. The Vincent Thomas Bridge in the Los Angeles metropolitan area, is a critical artery for commercial traffic flow in and out of the Los Angeles Harbour, and is at risk in the seismically active Southern California region, particularly because it straddles the Palos Verdes fault zone. A combination of linear and nonlinear system identification techniques is employed to obtain a complete reduced-order, multi-input-multi-output (MIMO) dynamic model of the Vincent Thomas Bridge based on the dynamic response of the structure to the 1987 Whittier and 1994 Northridge earthquakes.

Starting with the available acceleration measurements (which consists of 15 accelerometers on the bridge structure and 10 accelerometers at various locations on its base), a multistage, time-domain identification procedure is applied to the data set to develop an equivalent nonlinear, multi-degree-of-freedom model. This self-starting identification method uses least-squares parameter estimation methods, combined with nonparametric identification techniques, to generate a reduced-order nonlinear mathematical model suitable for use in subsequent studies to predict, with good fidelity, the response of the bridge under arbitrary dynamic environments.

Results of this study yield measurements of the equivalent linear modal properties (frequencies, mode shapes and non-proportional damping) as well as quantitative measures of the extent and nature of nonlinear interaction forces arising from strong ground shaking. It is shown that, for the particular subset of observations used in the identification procedure, the apparent nonlinearities in the system restoring forces are quite significant, and they contribute substantially to the improved fidelity of the model. Also shown is the potential of the identification technique under discussion to detect slight changes in the structure's influence coefficients, which may be precursors to damage and degradation in the structure being monitored.

INTRODUCTION

A considerable amount of system identification and damage detection work has been performed on structures subjected to ambient excitations and earthquake excitations. For the most part these have been performed on relatively small highway overpass bridges, and multi-story buildings. This paper attempts to tackle the system identification problem for a long-span structure excited by multiple inputs during strong earthquake events. This problem poses challenges of performing system identification where the vibration response has a substantial nonlinear component, where the structure has multiple input excitations, and with measurements from a sensor array with low spatial resolution. These are very practical problems that demand increased attention from the civil engineering research community.

¹ Columbia University, New York, NY 10027, USA, smyth@civil.columbia.edu

² University of Southern California, Los Angeles, CA 90089, USA, masri@vivian2.usc.edu

³ University of Southern California, Los Angeles, CA 90089, USA, abdelg@rcf.usc.edu

⁴ University of Southern California, Los Angeles, CA 90089, USA, nigbor@usc.edu

THE VINCENT THOMAS BRIDGE AND ITS DYNAMIC MONITORING SYSTEM

The Vincent Thomas Bridge is located in San Pedro, California, and is a major transportation artery connecting Los Angeles with its harbour. It is a cable-suspension bridge, approximately 1850m long, consisting of a main span of approximately 457m, two suspended side spans of 154m each, and a ten-span approach of approximately 545m length on either end. The roadway accommodates four lanes of traffic. The bridge was completed in 1964, and in 1980, was instrumented with 26 accelerometers as part of a seismic upgrading project. Currently, the sensor network is maintained by the California Division of Mines and Geology through the California Strong Motion Instrumentation Program. Ten accelerometers measure motion at the superstructure footings, and fifteen accelerometers are distributed at various locations and in lateral, longitudinal and vertical directions about the superstructure itself. Figure 1 shows the locations and directions of all of the sensors. Notice that the eastern half of the bridge is more densely instrumented. This is because the analog recorder is housed in the eastern cable anchorage. Because the ground motion accelerometers were placed at locations on the footings of the superstructure, the effects of soil-structure interaction need not be considered in the system identification process. These measurements may be viewed as direct inputs into the superstructure, because they already include the effects of the soil structure interaction. This differs from the often-encountered scenario, where nearby free-field recordings are considered to be excitation input, and where soil-structure interaction effects must be considered in the identification process.

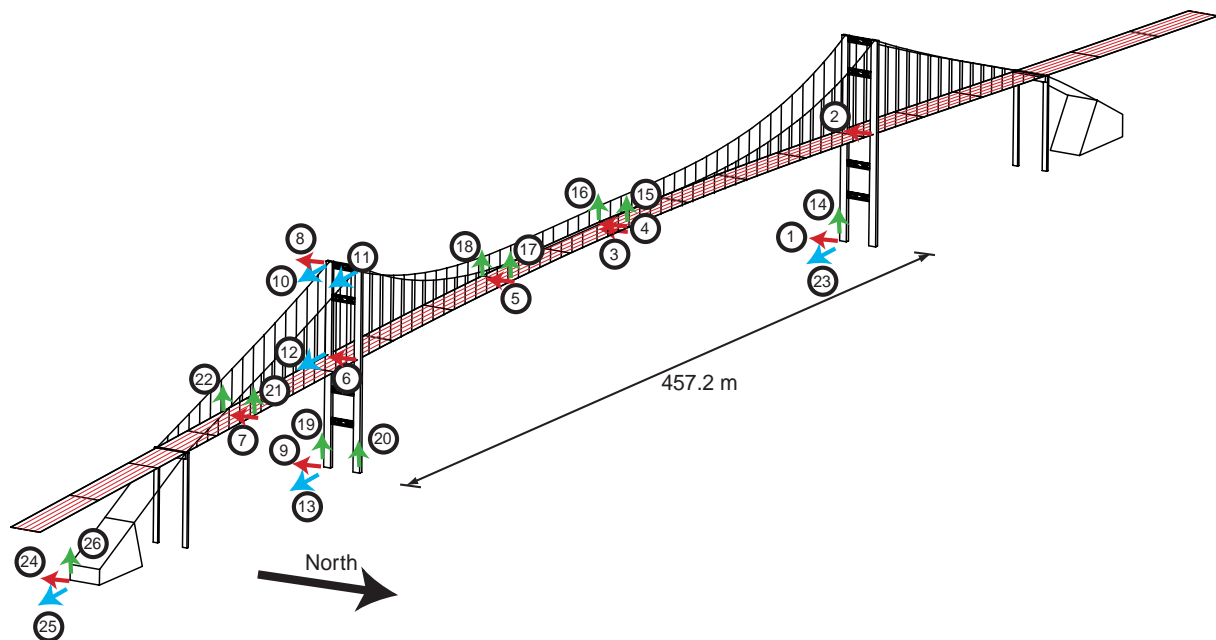


Figure 1: Accelerometer locations and directions for the instrumentation network on the Vincent Thomas Bridge

EARTHQUAKE RESPONSE DATA SETS

Since its installation, the instrumentation network has been triggered twice during large seismic events in southern California. The first was for the 1987 Whittier-Narrows earthquake ($M = 6.1$), and the second was for the 1994 Northridge earthquake ($M = 6.7$). The proximity of these earthquake epicenters relative to the Vincent Thomas Bridge is shown in Fig.2. Despite the greater distance to Northridge, because of the larger magnitude of that earthquake, the observed peak input and response accelerations ranged anywhere from 1.5 to 3 times of those recorded during the Whittier-Narrows earthquake.

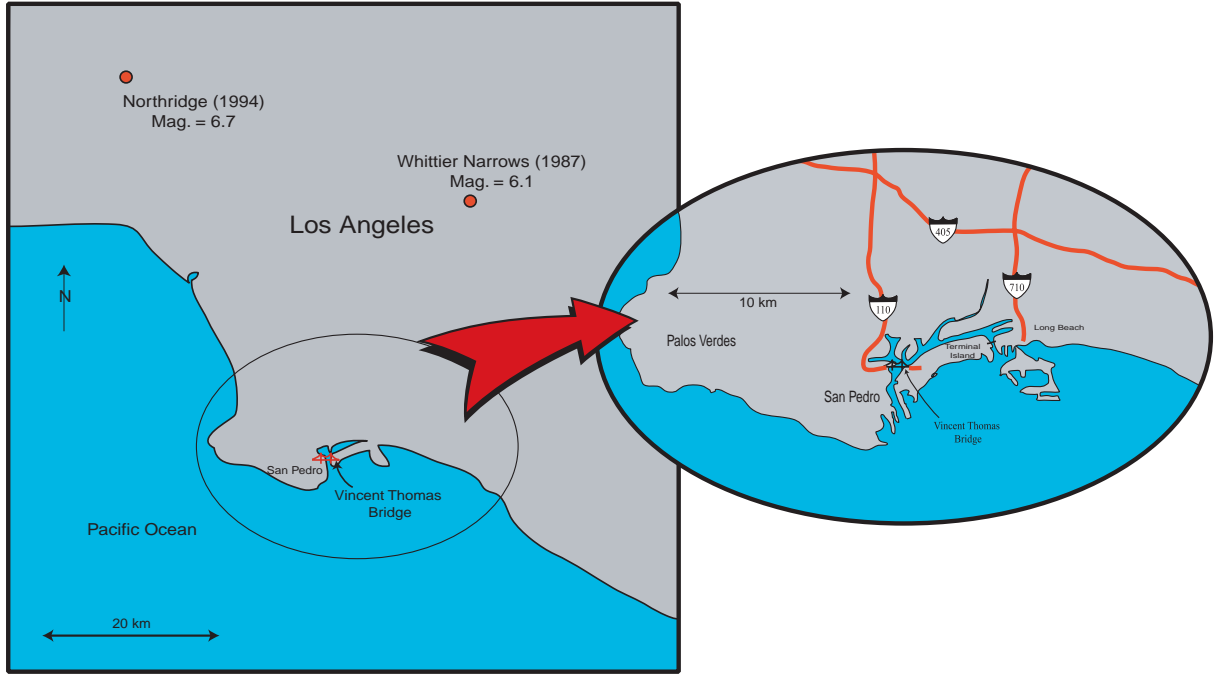


Figure 2: Map showing the location of the Vincent Thomas Bridge, and its proximity to the 1987 Whittier Narrows earthquake and the 1994 Northridge earthquake.

SYSTEM IDENTIFICATION PROCEDURE

The system identification procedure used in this study consists of two basic stages. The first is to identify a linear model, and the second, is to treat the unmodeled response not as error, but rather as nonlinear dynamics to be modeled. The first step involves the identification of an equivalent linear reduced order model of the structural system. In this case, because 15 structural response locations are available, the model will be a 15 DOF model with 10 support inputs. The equation of motion for such a system is given in Eq.(1), and is premultiplied by \mathbf{M}_{11}^{-1} . The \mathbf{M}_{11} , \mathbf{C}_{11} and \mathbf{K}_{11} matrices have the same meaning as the more typical \mathbf{M} , \mathbf{C} , \mathbf{K} notation of the mass, damping and stiffness matrices.

$$\mathbf{M}_{11}^{-1}\mathbf{C}_{11}\dot{\mathbf{X}}_1(t) + \mathbf{M}_{11}^{-1}\mathbf{K}_{11}\mathbf{X}_1 + \mathbf{M}_{11}^{-1}\mathbf{M}_{10}\ddot{\mathbf{X}}_0 + \mathbf{M}_{11}^{-1}\mathbf{C}_{10}\dot{\mathbf{X}}_0 + \mathbf{M}_{11}^{-1}\mathbf{K}_{10}\mathbf{X}_0 = -\mathbf{I}\ddot{\mathbf{X}}_1 \quad (1)$$

where $\mathbf{X}_1(t)$ = active degree-of-freedom (DOF) displacement vector of order n_1 , and $\mathbf{X}_0(t)$ = prescribed support displacement vector of order n_0 .

The parameters of the matrix clusters shown above are obtained by posing the problem as a series of overdetermined equations and then getting the unknown parameters by least-squares solution. This is easily done by writing each of the rows of the above equation of motion at every discrete time-step. If one assumes that the components in the mass, damping and stiffness matrices are the unknowns, then this is written generically as

$$\hat{\mathbf{R}}\hat{\mathbf{a}} = \hat{\mathbf{b}} \quad (2)$$

where

$$\hat{\mathbf{R}} \equiv \begin{bmatrix} \mathbf{R} & \mathbf{0} & \cdots & \mathbf{0} \\ \mathbf{0} & \mathbf{R} & & \\ \vdots & & \ddots & \\ \mathbf{0} & & & \mathbf{R} \end{bmatrix} \quad \hat{\boldsymbol{\alpha}} \equiv \begin{bmatrix} \boldsymbol{\alpha}_1 \\ \boldsymbol{\alpha}_2 \\ \vdots \\ \boldsymbol{\alpha}_{n_1} \end{bmatrix} \quad \hat{\mathbf{b}} \equiv \begin{bmatrix} \mathbf{b}_1 \\ \mathbf{b}_2 \\ \vdots \\ \mathbf{b}_{n_1} \end{bmatrix}$$

$n_1 N$ by $n_1(2n_1+3n_0)$ $n_1(2n_1+3n_0)$ by 1 $n_1 N$ by 1

Equation (2) may be formulated in several ways depending upon the assumptions which are made or upon *a priori* knowledge of certain parameters in the system matrices (Masri *et al.*, 1987). In this study there was no *a priori* knowledge, and the $\hat{\boldsymbol{\alpha}}$ parameter vector is assumed to either contain coefficients of symmetric or unsymmetric system matrices. When symmetric conditions are imposed, the $\hat{\boldsymbol{\alpha}}$ vector has less parameters, and the $\hat{\mathbf{R}}$ matrix must be constructed in a very particular order whose presentation is beyond the scope of this brief paper. The unsymmetric case is however quite simple to present, where Eq.(2) can be decomposed into

$$\mathbf{R}\boldsymbol{\alpha}_i = \mathbf{b}_i, \quad i = 1, n_1 \quad (3)$$

where

$$\mathbf{R} = \begin{bmatrix} \dot{X}_{11}(t_1) \dot{X}_{12}(t_1) \cdots \dot{X}_{1n_1}(t_1) & X_{11}(t_1) X_{12}(t_1) \cdots X_{1n_1}(t_1) & \ddot{X}_{01}(t_1) \ddot{X}_{02}(t_1) \cdots \ddot{X}_{0n_0}(t_1) & \dot{X}_{01}(t_1) \dot{X}_{02}(t_1) \cdots \dot{X}_{0n_0}(t_1) & X_{01}(t_1) X_{02}(t_1) \cdots X_{0n_0}(t_1) \\ \dot{X}_{11}(t_2) \dot{X}_{12}(t_2) \cdots \dot{X}_{1n_1}(t_2) & X_{11}(t_2) X_{12}(t_2) \cdots X_{1n_1}(t_2) & \ddot{X}_{01}(t_2) \ddot{X}_{02}(t_2) \cdots \ddot{X}_{0n_0}(t_2) & \dot{X}_{01}(t_2) \dot{X}_{02}(t_2) \cdots \dot{X}_{0n_0}(t_2) & X_{01}(t_2) X_{02}(t_2) \cdots X_{0n_0}(t_2) \\ \dot{X}_{11}(t_3) \dot{X}_{12}(t_3) \cdots \dot{X}_{1n_1}(t_3) & X_{11}(t_3) X_{12}(t_3) \cdots X_{1n_1}(t_3) & \ddot{X}_{01}(t_3) \ddot{X}_{02}(t_3) \cdots \ddot{X}_{0n_0}(t_3) & \dot{X}_{01}(t_3) \dot{X}_{02}(t_3) \cdots \dot{X}_{0n_0}(t_3) & X_{01}(t_3) X_{02}(t_3) \cdots X_{0n_0}(t_3) \\ \vdots & \vdots & \vdots & \vdots & \vdots \\ \dot{X}_{11}(t_N) \dot{X}_{12}(t_N) \cdots \dot{X}_{1n_1}(t_N) & X_{11}(t_N) X_{12}(t_N) \cdots X_{1n_1}(t_N) & \ddot{X}_{01}(t_N) \ddot{X}_{02}(t_N) \cdots \ddot{X}_{0n_0}(t_N) & \dot{X}_{01}(t_N) \dot{X}_{02}(t_N) \cdots \dot{X}_{0n_0}(t_N) & X_{01}(t_N) X_{02}(t_N) \cdots X_{0n_0}(t_N) \end{bmatrix}$$

$n_1=15$ columns $n_1=15$ columns $n_0=10$ columns $n_0=10$ columns $n_0=10$ columns
 $2n_1+3n_0=60$ columns

$$\mathbf{b}_i = \left[-\ddot{X}_{1i}(t_1), -\ddot{X}_{1i}(t_2), -\ddot{X}_{1i}(t_3), \dots, -\ddot{X}_{1i}(t_N) \right]^T, \quad i = 1, n_1$$

$$\boldsymbol{\alpha}_i = \left[\left\langle {}^2\mathbf{A}_i \right\rangle, \left\langle {}^3\mathbf{A}_i \right\rangle, \left\langle {}^3\mathbf{A}_i \right\rangle, \left\langle {}^4\mathbf{A}_i \right\rangle, \left\langle {}^5\mathbf{A}_i \right\rangle \right]^T, \quad i = 1, n_1$$

$${}^2\mathbf{A} = \mathbf{M}_{11}^{-1}\mathbf{C}_{11}$$

$${}^3\mathbf{A} = \mathbf{M}_{11}^{-1}\mathbf{K}_{11}$$

$${}^4\mathbf{A} = \mathbf{M}_{11}^{-1}\mathbf{M}_{10}$$

$${}^5\mathbf{A} = \mathbf{M}_{11}^{-1}\mathbf{C}_{10}$$

$${}^6\mathbf{A} = \mathbf{M}_{11}^{-1}\mathbf{K}_{10}$$

With Eq.(2) or Eq.(3) one can solve for the unknown parameter vectors $\hat{\boldsymbol{\alpha}}$ or the $\boldsymbol{\alpha}_i$'s by obtaining the pseudoinverse of the $\hat{\mathbf{R}}$ or \mathbf{R} matrices, respectively. This can be written as follows

$$\boldsymbol{\alpha} = \hat{\mathbf{R}}^\dagger \hat{\mathbf{b}} \quad \text{or} \quad \boldsymbol{\alpha}_i = \mathbf{R}^\dagger \mathbf{b}_i \quad (4)$$

where \dagger stands for the pseudoinverse of a matrix. Now that the unknown system matrix coefficients have been determined they may be inserted into either Eq.(2) or Eq.(3) to yield an estimated \mathbf{b} vector, \mathbf{b}^{est} , which simply contains estimates of the accelerations of the active degrees of freedom. Rather than treating the difference $(\mathbf{b} - \mathbf{b}^{est})$ as modeling error, we treat it as a nonlinear residual, \mathbf{b}_{nl} , to be modeled. There are several nonlinear modeling techniques available to us, however a nonparametric technique was chosen here. Each residual in acceleration was fitted by forming a set of basis functions from the measured displacements and velocities of the active degrees of freedom and the accelerations of the base (Smyth, 1998). These basis functions were generated by producing all possible 3rd order power combinations of all of these signals. These were then arranged just as in Eq.(4) (where only 1st order, i.e., linear model, basis functions were assumed) and a new set of unknown coefficients was identified.

APPLICATION OF THE SYSTEM IDENTIFICATION TECHNIQUE

Equivalent Linear System Identification from Bridge Response Data

It is not surprising that, given the highly nonstationary nature of earthquake ground motions, the measurements of base and structural accelerations were also highly nonstationary for both earthquake events. From preliminary analysis, it was also suspected that during the time of strongest shaking, the response had a significant nonlinear component. This may have been due to several factors including geometric nonlinearities caused by large deformations, or perhaps banging of expansion joints in the bridge deck. With this in mind, one must be careful of the conclusions which are drawn from this type of relatively autonomous equivalent linearization technique. Because different levels of nonlinearity were suspected to exist during different periods of shaking, identification could be performed on various time windows of the recorded measurements. A sample result showing the identified system modal frequencies for both of the data sets is shown in Fig. (3). In this case the entire record lengths were used for the time-domain based identification procedure under discussion.

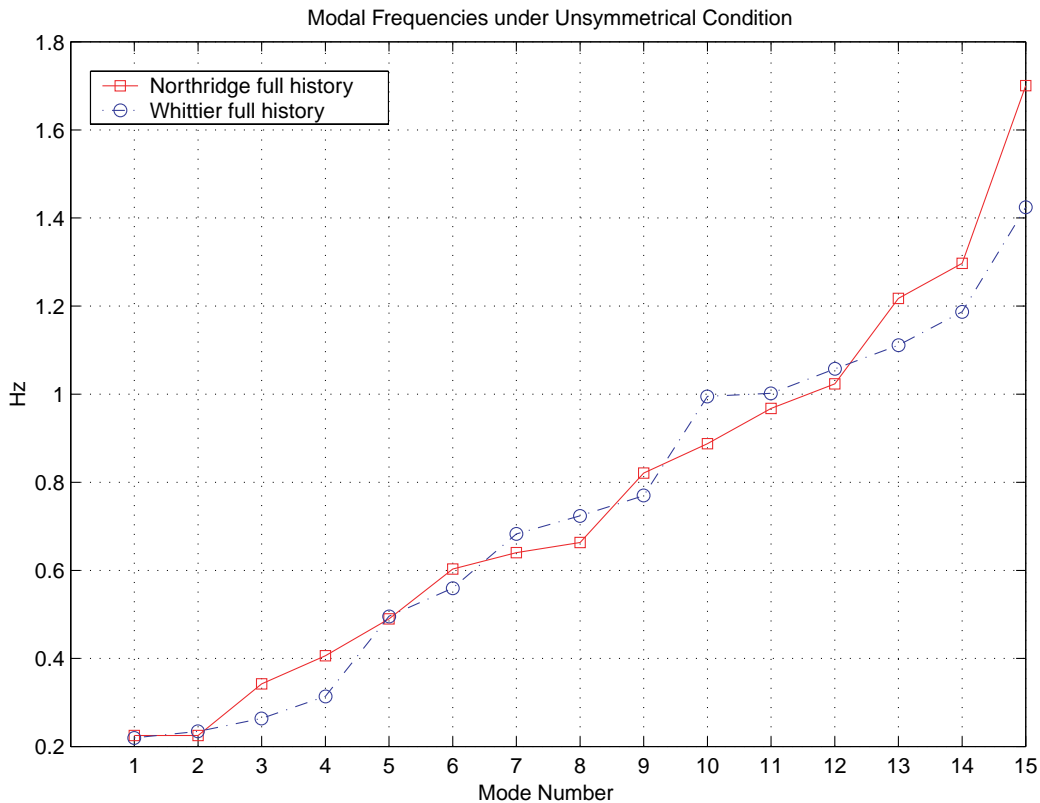


Figure 3: Identified modal frequencies for the reduced order equivalent linear model based on the Northridge and Whittier-Narrows earthquake response data recordings.

Clearly there are some similarities in the identified modal frequencies, and there are some differences. It is important to stress that, unlike many methods which yield only modal frequencies and damping estimates, these quantities are actually computed indirectly after the complete system matrices are identified. In fact, the identification procedure makes no assumption of classical normal modes, and thus we get information on the nonproportional damping. Unfortunately, however, because this is a base motion input case, and not a force excited example, it is only possible to identify the cluster of system matrices premultiplied by the inverse of the mass matrix.

Because the identification is relatively unconstrained, and because the equivalent linear modeling is being performed on what is suspected to be nonlinear response dynamics, there is nothing to prevent the identification of negative damping coefficients. This would detract from the method if only used for modal analysis. Table 1 shows the damping ratios of the equivalent linear systems identified for each earthquake.

Table 1: Comparison of identified modal frequencies and damping ratios for equivalent linear dynamic models based on the Northridge and Whittier-Narrows bridge response recording. Note that only the second half of the records was used for this sample result.

Mode	Sym. ID Northridge Frequency (Hz)	Sym. ID Northridge Damping Ratio	Sym. ID Whittier Frequency (Hz)	Sym. ID Whittier Damping Ratio
1	0.2267	0.0013	0.2536	-0.0457
2	0.3325	-0.0395	0.2562	0.2011
3	0.4312	-0.0310	0.3023	-0.0947
4	0.4429	0.0206	0.5529	-0.2072
5	0.4631	0.0058	0.5737	0.0305
6	0.4768	0.0570	0.6322	0.0232
7	0.5046	0.0359	0.7180	0.0079
8	0.5679	0.0336	0.8146	-0.0375
9	0.6342	0.0539	0.8152	0.0304
10	0.6942	0.0109	0.8524	-0.0091
11	0.8374	0.0530	0.9556	-0.0083
12	0.9535	-0.0147	1.0466	0.0019
13	0.9802	-0.0369	1.0842	0.0502
14	1.0342	0.0281	1.1270	0.0196
15	1.0558	0.0142	1.3895	0.0091

Nonparametric Modeling of the Nonlinear Residual

Depending upon which time window was used for equivalent linear modeling and subsequent comparison of fits, the nonlinear residual error ranged anywhere from as low as 10% to as high as 85%, with an average residual of about 50-60%. A sample of these fitting errors is shown below in Fig.(4).

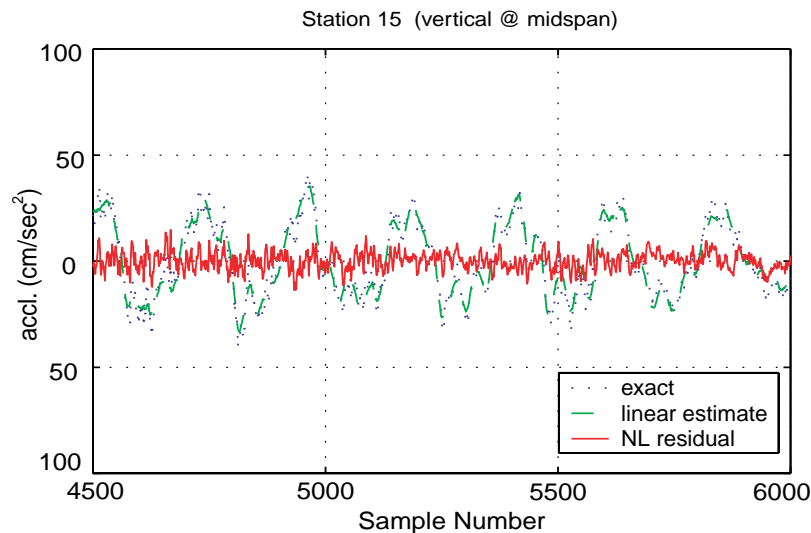


Figure 4: Comparison of the acceleration fit for the equivalent linear model and the exact measured time-history for station 15, which is a vertical motion at the midspan of the bridge.

Notice in Fig.(4) how the acceleration based on the linear model matches the response reasonably well (approximately 20% rms residual). This is largely attributable to the fact that the vertical deck modes dominated the response signal for this station, and were relatively easy for the linear system to model.

Nonlinear residuals remain for each active degree of freedom acceleration measurement. These were fitted with the nonparametric technique outlined earlier. An example of the performance of this method is shown in Fig.(5). In this case the fitting was performed on lateral response station 7, which had a 46% rms nonlinear residual to be modeled nonparametrically. The fitting of this nonlinear component was to within 55% rms error. Therefore the entire signal was modeled to within an accuracy of about 25.3% error. This is a respectable result given that the system is undergoing change during the excitation.

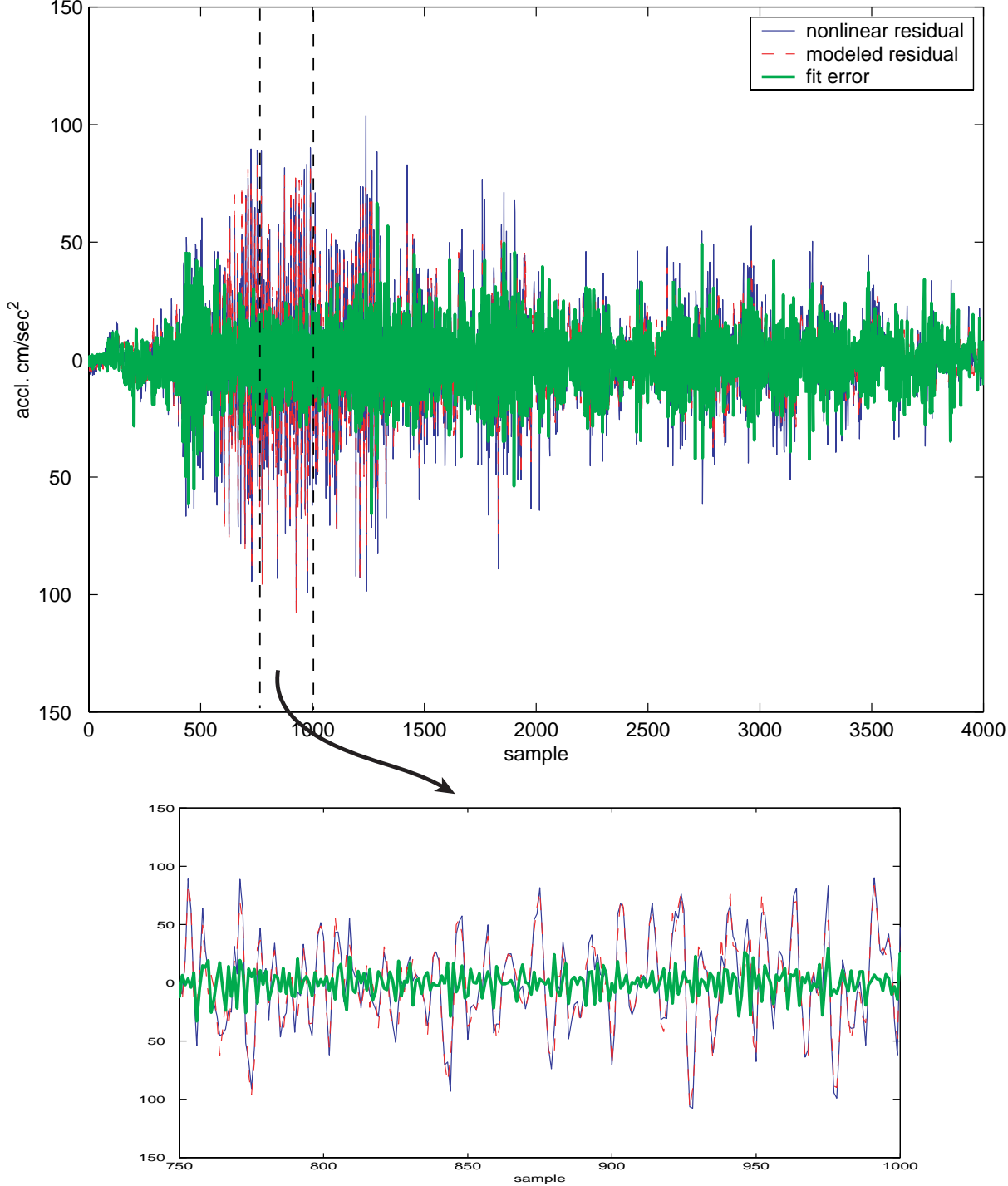


Figure 5: Comparison of the nonlinear residual component of the station 7 measurement (solid blue line), the nonparametrically modeled signal (dashed red line), and the fitting error (thick green line).

DISCUSSION

A brief sample of the identification results has been shown here, and they confirm that this relatively simple time-domain based identification procedure can capture, in a reduced order model, the essence of the response dynamics of this highly complex structural system. The equivalent linear identification phase yields system information which includes complex mode shapes; in other words, it makes no assumptions of proportional damping. The modal frequencies obtained for the two earthquakes are similar, but indicate some system changes. Additional analysis is needed to compare these identified systems under earthquake loading with previous identification work performed on the bridge under ambient loading conditions (Abdel-Ghaffar and Housner, 1977, Abdel-Ghaffar *et al.*, 1995).

To give some idea of the variation over time in the system dynamics, histogram plots of the identified ${}^3\mathbf{A}(10,10)$ parameter are shown in Fig.(6). Recall that the ${}^3\mathbf{A}$ matrix represents $\mathbf{M}_{11}^{-1}\mathbf{K}_{11}$, and therefore if one assumes the mass distribution does not vary, this reflects variation in the stiffness matrix. The distribution was obtained by performing the identification procedure over short windows (1000 pts. for Whittier, and 1500 pts. for Northridge) and shifting the windows by small amounts until the end of the data set was reached. These types of results can be compiled to track structural changes during the excitation process.

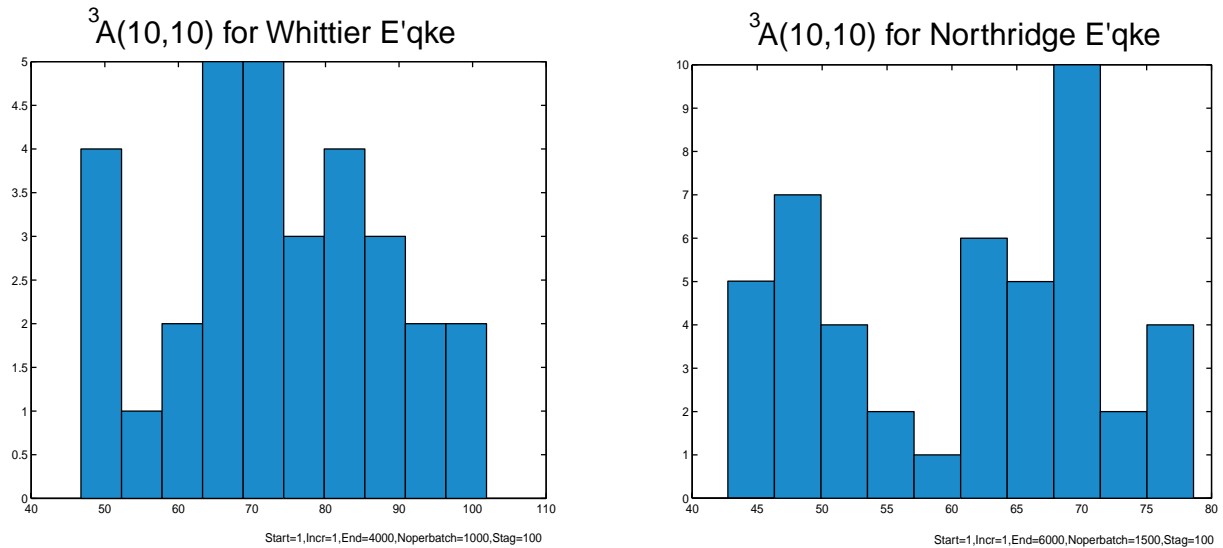


Figure 6: Histograms showing variation in a sample coefficient of the equivalent linear models from both earthquake data sets. The variation was produced by performing the identification at numerous shifted windows in the measurement time-histories.

References

- Masri, S.F., Miller, R.K., Saud, A.F., and Caughey, T.K., (1987), "Identification of nonlinear vibrating structures: part I – formulation; part II - applications" *Jo. of Applied Mechanics*, 54, pp. 918-929.
- Smyth, A.W., (1998), "Analytical and experimental studies in system identification and monitoring in the context of structural control," *Ph.D. Dissertation*, University of Southern California, Los Angeles.
- Abdel-Ghaffar, A.M., and Housner, G.W., (1977), "An analysis of the dynamic characteristics of a suspension bridge by ambient vibration measurements," *Earthquake Engineering Research Laboratory*, California Institute of Technology, Report EERL 77-01.
- Abdel-Ghaffar, A.M., Masri, S.F., and Nigbor, R.N., (1995), "Preliminary report on the Vincent Thomas Bridge monitoring test," *Center for Research in Earthquake and Construction Engineering*, University of Southern California, Report No. M9510.